

学位論文(要約)

# Molecular Gas in Late-stage Merging Galaxies

(衝突末期段階の銀河における分子ガスの観測的研究)

平成25年12月 博士(理学)

申請

東京大学大学院理学系研究科

天文学専攻

植田 準子



# Abstract

We reveal the distribution and kinematics of molecular gas in colliding galaxy systems near the late-stage of their coalescence, called merger remnants. We statistically analyze their properties utilizing the largest-to-date survey of cold molecular gas. This is the first step in our series of studies which put emphasis on molecular gas in merger remnants.

It has been long predicted from numerical simulations that a major merger of two disk galaxies results in the formation of a spheroid-dominated early-type galaxy. Contrary to this classical scenario of galaxy merger evolution, recent simulations that include more realistic gas physics have shown that not all of the major mergers will become early-type galaxies, but some will re-emerge as a disk-dominated late-type galaxy. However there has been no observational confirmation of this theoretical prediction. In order to verify this scenario and to investigate the evolution of galaxy after a merging event, we have conducted a  $^{12}\text{CO}$  imaging survey of optically-selected merger remnants in the local Universe using millimeter/submillimeter interferometers including ALMA, SMA, and CARMA, and the NRO 45 m single-dish telescope.

We find that 65 % (24/37) of the sample show kinematical signatures of a rotating molecular gas disk. We reveal a high occurrence of molecular gas disks including rings in the merger remnants, and the sizes of these disks vary significantly from 1.1 kpc to 9.3 kpc. We estimate the size ratio ( $R_{\text{ratio}}$ ) of the gas disk to the stellar spheroidal component for 24 merger remnants with gas disks in order to investigate whether cold molecular gas disks are in extended form, as predicted from recent numerical simulations. The size ratios  $R_{\text{ratio}}$  for 54 % (13/24) of the merger remnants are less than unity. Six merger remnants which are bright at infrared wavelengths have compact molecular gas disks, which may have formed by past gas inflow that was triggered by dynamical instability following the merging. On the other hand, 46 % (11/24) of the merger remnants have gas disks which are extended relative to the stellar components. We also discover a possible positive correlation between  $R_{\text{ratio}}$

---

and the total far-infrared luminosity. This suggests that the physical activities that are responsible for increasing luminosity, namely starburst/AGN, are related to the formation of the extended molecular gas disks. The molecular gas disks in the merger remnants show various properties, and we conclude that our sample includes merger remnants at different stages of their evolution, whose progenitors have different characteristics or which have different initial conditions.

From comparisons of the merger remnants with early-type galaxies and late-type galaxies regarding their molecular gas and stellar components, overall, our conclusion is that 65 % of the merger remnants evolve into early-type galaxies, 5 % into late-type galaxies, 14 % into either early-type/late-type galaxies, and 16 % into galaxies which cannot be classified into early-type/late-type galaxies. Among the sources with observational signatures of a rotating molecular gas disk, we find that sources with compact molecular gas disks will become early-type galaxies regardless of the gas mass fraction, mainly because of the short depletion time of the molecular gas ( $\lesssim 10^8$  yr) and high gas concentration in the nuclear region. On the other hand, we find that sources with extended molecular gas disks and large gas mass fractions are likely to become late-type galaxies, unless there are further mechanisms which transport the molecular gas toward the central regions thereby decreasing the sizes of the gas disks. Confirming the evolution path of the sources with extended molecular gas disks and low gas mass fractions requires further studies to investigate whether a large amount of cold gas will settle on the extended gas disks by the returning of the ejected cold gas via tidal tails and cold gas stream/accretion. For six merger remnants whose velocity fields cannot be modeled with circular motion, their clumpy morphology and complex gas structure are different from the morphology and structure of both early-type/late-type galaxies, therefore their evolution path is not clear. The seven merger remnants which were not detected in the CO line will evolve into early-type galaxies earlier than the merger remnants with compact molecular gas disks.

This study confirms, observationally, a new scenario that merging events are the crossroads of galaxy evolution, reprocessing them into a mixture of types including early-type/late-type galaxies.

# Contents

<b>Abstract</b>	<b>I</b>
<b>1 Introduction</b>	<b>1</b>
1.1 Extragalactic Astronomy through Observations . . . . .	2
1.2 Galaxy Classification . . . . .	4
1.2.1 Morphological Classification . . . . .	4
1.2.2 Starburst Galaxies . . . . .	6
1.2.3 Ultra/Luminous Infrared Galaxies . . . . .	6
1.3 Galaxy Mergers . . . . .	7
1.3.1 Overview . . . . .	7
1.3.2 Merger Classification . . . . .	8
1.3.3 Merger Sequence and Timescale . . . . .	9
1.4 Galaxy Formation and Evolution . . . . .	10
1.4.1 Galaxy Formation in the $\Lambda$ -CDM model . . . . .	10
1.4.2 Galaxy Evolution through Galaxy Mergers . . . . .	12
1.5 Merger Remnants . . . . .	13
1.5.1 Previous Studies on Merger Remnants . . . . .	15
1.5.2 The Evolution of Merger Remnants . . . . .	16
1.6 Radio Astronomy and Interferometry . . . . .	16
1.6.1 Radio Observations in the CO line . . . . .	17
1.6.2 Radio Interferometer . . . . .	17
1.7 Scientific Goals and Thesis Structure . . . . .	20

<b>2</b>	<b>Merger Remnant CO Imaging Survey</b>	<b>23</b>
2.1	Merger Remnant Sample . . . . .	24
2.2	Observations and Data Reduction . . . . .	29
2.2.1	Observations with ALMA . . . . .	29
2.2.2	Observations with SMA . . . . .	29
2.2.3	Observations with CARMA . . . . .	29
2.2.4	Interferometric Archival Data . . . . .	30
2.2.5	Single-dish Observations . . . . .	30
2.3	Distribution and Kinematics of the Molecular Gas . . . . .	33
2.3.1	High Resolution Interferometric CO Maps . . . . .	33
2.3.2	Single-dish CO (1–0) Spectra . . . . .	36
2.3.3	The Molecular Gas Disks in Merger Remnants . . . . .	40
<b>3</b>	<b>Global Properties of the Molecular Gas in Merger Remnants</b>	<b>43</b>
3.1	The Extent of the Molecular Gas . . . . .	44
3.2	The Relative Size of the Molecular Gas Extent . . . . .	47
3.3	The Structural Parameters of the Molecular Disks . . . . .	50
3.4	Molecular Gas Mass in Merger Remnants . . . . .	52
3.5	Star Formation Activity . . . . .	54
3.5.1	The Integrated Star-Formation Rate . . . . .	54
3.5.2	The Depletion Time of the Molecular Gas . . . . .	55
3.6	Possibility of Active Galactic Nuclei . . . . .	56
3.7	Summary of the Global Properties of the Merger Remnants . . . . .	58
3.8	Individual Sources . . . . .	60
3.8.1	UGC 6 (VV 806, Mrk 334) . . . . .	60
3.8.2	NGC 34 (NGC 17, VV 850, Mrk 938) . . . . .	60
3.8.3	Arp 230 (IC 51) . . . . .	61
3.8.4	NGC 455 (Arp 164, UGC 815) . . . . .	62
3.8.5	NGC 828 (UGC 1655) . . . . .	62
3.8.6	UGC 2238 . . . . .	63
3.8.7	NGC 1210 (AM 0304–255) . . . . .	63

3.8.8	AM 0318–230 . . . . .	64
3.8.9	Arp 187 . . . . .	64
3.8.10	AM 0612–373 . . . . .	64
3.8.11	UGC 4079 (Mrk 84) . . . . .	64
3.8.12	AM 0956–282 (VV 592) . . . . .	65
3.8.13	AM 1158–333 . . . . .	65
3.8.14	NGC 4441 (UGC 7572) . . . . .	66
3.8.15	AM 1255–430 . . . . .	66
3.8.16	NGC 5018 . . . . .	67
3.8.17	AM 1419–263 . . . . .	67
3.8.18	UGC 9829 (VV 847) . . . . .	68
3.8.19	NGC 6052 (Arp 209, UGC 10182, VV 86, Mrk 297) . . . . .	68
3.8.20	UGC 10675 (VV 805, Mrk700) . . . . .	69
3.8.21	AM 2038–382 . . . . .	69
3.8.22	AM 2055–425 . . . . .	69
3.8.23	NGC 7135 (AM 2146–350, IC 5136) . . . . .	70
3.8.24	NGC 7252 (Arp 226, AM 2217-245) . . . . .	71
3.8.25	AM 2246–490 . . . . .	71
3.8.26	NGC 7585 (Arp 223) . . . . .	72
3.8.27	NGC 7727 (Arp 222, VV 67) . . . . .	72
<b>4</b>	<b>The Evolution of the Merger Remnants</b>	<b>75</b>
4.1	Control Sample . . . . .	76
4.1.1	Early-type Galaxies in the ATLAS <sup>3D</sup> sample . . . . .	76
4.1.2	Late-type Galaxies in the BIMA SONG sample . . . . .	77
4.2	The Absolute Size of the Molecular Gas Disk . . . . .	77
4.3	The Relative Size of the Molecular Gas Disk . . . . .	79
4.4	The Gas Mass Fraction . . . . .	82
4.5	Relation between the size of the gas disk and gas mass fraction . . . . .	84
4.6	Evolution of Merger Remnants . . . . .	91
4.6.1	Type A . . . . .	93

4.6.2	Type B: Unclassified . . . . .	96
4.6.3	Type C: ETG candidates . . . . .	96
4.7	Summary of the evolution of the merger remnants . . . . .	97
<b>5</b>	<b>Summary and Future Prospects</b>	<b>103</b>
5.1	Summary . . . . .	103
5.2	Future Prospects: What's next? . . . . .	106
	<b>Appendix</b>	<b>108</b>
<b>A</b>	<b>Channel Maps</b>	<b>109</b>
<b>B</b>	<b>Position-Velocity Diagram</b>	<b>143</b>
<b>C</b>	<b>Fitting and Modeling Tests for the Reproducibility of Velocity Fields</b>	<b>157</b>
C.1	TEST 1: Initial Values . . . . .	157
C.2	TEST 2: Fitting with Concentric Rings . . . . .	161
C.3	TEST 3: Non-Elliptical Structure . . . . .	162
<b>D</b>	<b>Basic Definitions</b>	<b>167</b>
D.1	Intensity and Flux Density . . . . .	167
D.2	Brightness Temperature . . . . .	169
D.3	The CO Line Luminosity . . . . .	171
D.4	The CO Luminosity-to-H <sub>2</sub> Mass Conversion Factor . . . . .	173
<b>E</b>	<b>The Kolmogorov-Smirnov Test</b>	<b>175</b>
	<b>Bibliography</b>	<b>177</b>
	<b>Acknowledgement</b>	<b>188</b>



# List of Figures

1.1	An example of multi-wavelength observations . . . . .	3
1.2	Hubble’s tuning fork for galaxy classification . . . . .	5
1.3	Merger rate as a function of redshift . . . . .	8
1.4	Merger sequence and timescale . . . . .	9
1.5	The evolution and formation of the dark-matter halo . . . . .	11
1.6	The simulation resulted in reformation of an extended gas disk . . . . .	14
1.7	The surviving disk fraction as a fraction of gas mass fractions . . . . .	14
1.8	Existing millimeter/submillimeter interferometers . . . . .	19
2.1	K-band images of the 37 merger remnant sample . . . . .	26
2.2	The CO integrated intensity maps of 30 merger remnants . . . . .	34
2.3	The CO velocity fields of 30 merger remnants. . . . .	35
2.4	The CO (1–0) spectra of 10 merger remnants . . . . .	37
3.1	Histogram of the molecular gas extent . . . . .	45
3.2	Relation between the molecular gas extent and $1 \sigma$ mass sensitivity . . . . .	45
3.3	Histogram of the relative size of the molecular gas extent . . . . .	48
3.4	Relation between the FIR luminosity and the relative size of the molecular gas extent . . . . .	48
3.5	Histogram of the asymmetry parameter . . . . .	51
3.6	Histogram of the concentration parameter . . . . .	51
3.7	The $q$ -values (The radio-FIR correlation) . . . . .	57
4.1	Histogram of the absolute size of the molecular gas disk . . . . .	78
4.2	Histogram of the relative size of the molecular gas disk . . . . .	81

4.3	Histogram of the gas mass fraction . . . . .	83
4.4	Relation between the gas mass fraction and relative size of the molecular gas disk . . .	85
4.5	Relation between the gas mass fraction and disk size (divided by the stellar mass) . . .	87
4.6	The predicted change of the gas mass fraction . . . . .	89
4.7	Classification chart of the merger remnants. . . . .	91
4.8	The determination of the boundary of two distributions . . . . .	92
4.9	Four sub-types of Type A . . . . .	93
A.1	Channel Maps of UGC 6 . . . . .	109
A.2	Channel Maps of NGC 34 . . . . .	110
A.3	Channel Maps of Arp 230 . . . . .	111
A.4	Channel Maps of NGC 828 . . . . .	112
A.5	Channel Maps of UGC 2238 . . . . .	113
A.6	Channel Maps of NGC 1614 . . . . .	114
A.7	Channel Maps of Arp 187 . . . . .	115
A.8	Channel Maps of AM 0612-373 . . . . .	117
A.9	Channel Maps of NGC 2623 . . . . .	119
A.10	Channel Maps of NGC 2782 . . . . .	120
A.11	Channel Maps of UGC 5101 . . . . .	122
A.12	Channel Maps of AM 0956-282 . . . . .	123
A.13	Channel Maps of NGC 3256 . . . . .	124
A.14	Channel Maps of NGC 3597 . . . . .	125
A.15	Channel Maps of AM 1158-333 . . . . .	126
A.16	Channel Maps of NGC 4194 . . . . .	127
A.17	Channel Maps of NGC 4441 . . . . .	128
A.18	Channel Maps of UGC 8058 . . . . .	130
A.19	Channel Maps of AM 1255-430 . . . . .	131
A.20	Channel Maps of AM 1300-233 . . . . .	132
A.21	Channel Maps of Arp 193 . . . . .	133
A.22	Channel Maps of UGC 9829 . . . . .	134
A.23	Channel Maps of NGC 6052 . . . . .	135

A.24 Channel Maps of UGC 10675 . . . . .	136
A.25 Channel Maps of AM 2038-382 . . . . .	137
A.26 Channel Maps of AM 2055-425 . . . . .	138
A.27 Channel Maps of NGC 7135 . . . . .	139
A.28 Channel Maps of NGC 7252 . . . . .	140
A.29 Channel Maps of AM 2246-490 . . . . .	141
A.30 Channel Maps of NGC 7727 . . . . .	142
B.1 Position-Velocity diagram of UGC 6 . . . . .	143
B.2 Position-Velocity diagram of NGC 34 . . . . .	144
B.3 Position-Velocity diagram of Arp 230 . . . . .	144
B.4 Position-Velocity diagram of NGC 828 . . . . .	145
B.5 Position-Velocity diagram of UGC 2238 . . . . .	145
B.6 Position-Velocity diagram of NGC 1614 . . . . .	146
B.7 Position-Velocity diagram of Arp 187 . . . . .	146
B.8 Position-Velocity diagram of AM 0612-373 . . . . .	147
B.9 Position-Velocity diagram of NGC 2623 . . . . .	147
B.10 Position-Velocity diagram of NGC 2782 . . . . .	148
B.11 Position-Velocity diagram of UGC 5101 . . . . .	148
B.12 Position-Velocity diagram of AM 0956-282 . . . . .	149
B.13 Position-Velocity diagram of NGC 3256 . . . . .	149
B.14 Position-Velocity diagram of NGC 3597 . . . . .	150
B.15 Position-Velocity diagram of NGC 4441 . . . . .	150
B.16 Position-Velocity diagram of UGC 8058 . . . . .	151
B.17 Position-Velocity diagram of AM 1300-233 . . . . .	151
B.18 Position-Velocity diagram of Arp 193 . . . . .	152
B.19 Position-Velocity diagram of UGC 10675 . . . . .	152
B.20 Position-Velocity diagram of AM 2038-382 . . . . .	153
B.21 Position-Velocity diagram of AM 2055-425 . . . . .	153
B.22 Position-Velocity diagram of NGC 7252 . . . . .	154
B.23 Position-Velocity diagram of AM 2246-490 . . . . .	154

B.24 Position-Velocity diagram of NGC 7727 . . . . . 155

C.1 The velocity field of MODEL 1 . . . . . 158

C.2 Fitting results of TEST 1 . . . . . 160

C.3 Fitting results of TEST 2 . . . . . 161

C.4 Fitting results of TEST 3 . . . . . 165

D.1 The definition of the specific Intensity . . . . . 168

D.2 Total flux from an uniformly bright sphere . . . . . 169

# List of Tables

2.1	Merger Remnant Sample . . . . .	28
2.2	Properties of Interferometric Observations . . . . .	31
2.3	Properties of Archival Interferometric Data . . . . .	32
2.4	The CO Properties Derived from Interferometric Maps . . . . .	38
2.5	Properties of Single-dish Observations and Archival Data . . . . .	39
2.6	Kinematical Parameters of the CO Velocity Field . . . . .	42
3.1	Structure Parameters of the CO Extent . . . . .	46
3.2	Global Properties of the Merger Remnant Sample (1) . . . . .	53
3.3	The Radio–FIR Correlation . . . . .	59
4.1	P-values for the Comparison of the Disk Sizes of the Molecular Gas . . . . .	80
4.2	P-values for the Comparison of the Gas Mass Fractions . . . . .	84
4.3	Global Properties of the Merger Remnant Sample (2) . . . . .	90
4.4	Average Properties of the Merger Remnants in Different Types . . . . .	99
4.5	Properties of the Early-type Galaxies in the ATLAS <sup>3D</sup> Sample . . . . .	100
4.6	Properties of the Late-type Galaxies in the BIMA SONG Sample (1) . . . . .	101
4.7	Properties of the Late-type Galaxies in the BIMA SONG Sample (2) . . . . .	102
C.1	Basic Parameters of MODEL 1 . . . . .	158
C.2	Fitting Results for TEST 1 . . . . .	159



# **Chapter 1**

## **Introduction**

## 1.1 Extragalactic Astronomy through Observations

There are more than 100 billion galaxies in the Universe, though we can see only four galaxies with our naked eyes. Galaxies are gravitationally bound systems composed of stars, star clusters, interstellar medium of gas and dust, and dark matter. The majority of galaxies are parts of larger associations known as groups, clusters, and superclusters of galaxies. Each individual galaxies have different size, mass, stellar population, and structure, which tell us about its evolutionary history.

Galaxies usually emit light at all wavelengths from X-rays to radio (Figure 1.1). We provide a brief summary about observations towards galaxies at different wavelengths.

- **Optical observations:** Initial observations towards galaxies were carried out using visible light, which traces mainly stars because the peak wavelength of most stars lies in the optical. Optical imaging reveals the stellar populations and the distribution of dusty regions via extinction. In addition, imaging with a narrow-band filter shows ionized HII regions in galaxies, which are usually coincident with star forming regions.
- **Infrared observations:** Infrared radiation can pass through dusty regions. Therefore infrared observations are useful for investigating objects obscured at visible wavelength by gas and dust. The infrared is divided into three spectral regions, near-, mid- and far-infrared. The near-infrared light is dominated by stars, but mainly tracing red giant stars and red dwarfs. The mid- and far-infrared light is produced by radiation from dust, which is heated by stars formed in molecular clouds. Far-infrared imaging is also used to discover high- $z$  galaxies.
- **Radio observations:** The continuum observations are used for examining activity in galactic nuclei, in particular active galactic nuclei (AGNs), and for investigating star forming activities. The atomic and molecular line observations, such as the neutral hydrogen line (HI line) at 21 cm and the CO (1–0) line at 115 GHz, are used for investigating the properties of gaseous components, such as chemical evolution and physical state. In addition, the HI line is useful for the kinematic measurements in galaxies (e.g., galactic rotation curve).
- **Ultraviolet and X-ray observations:** Ultraviolet (UV) and X-ray telescopes can detect high energy astrophysical phenomena. UV spectroscopy is used to discern the temperature, density and chemical composition of the interstellar medium. The X-ray spectrum is a powerful tool for identifying AGNs, because their luminosities are considerably higher than those of other



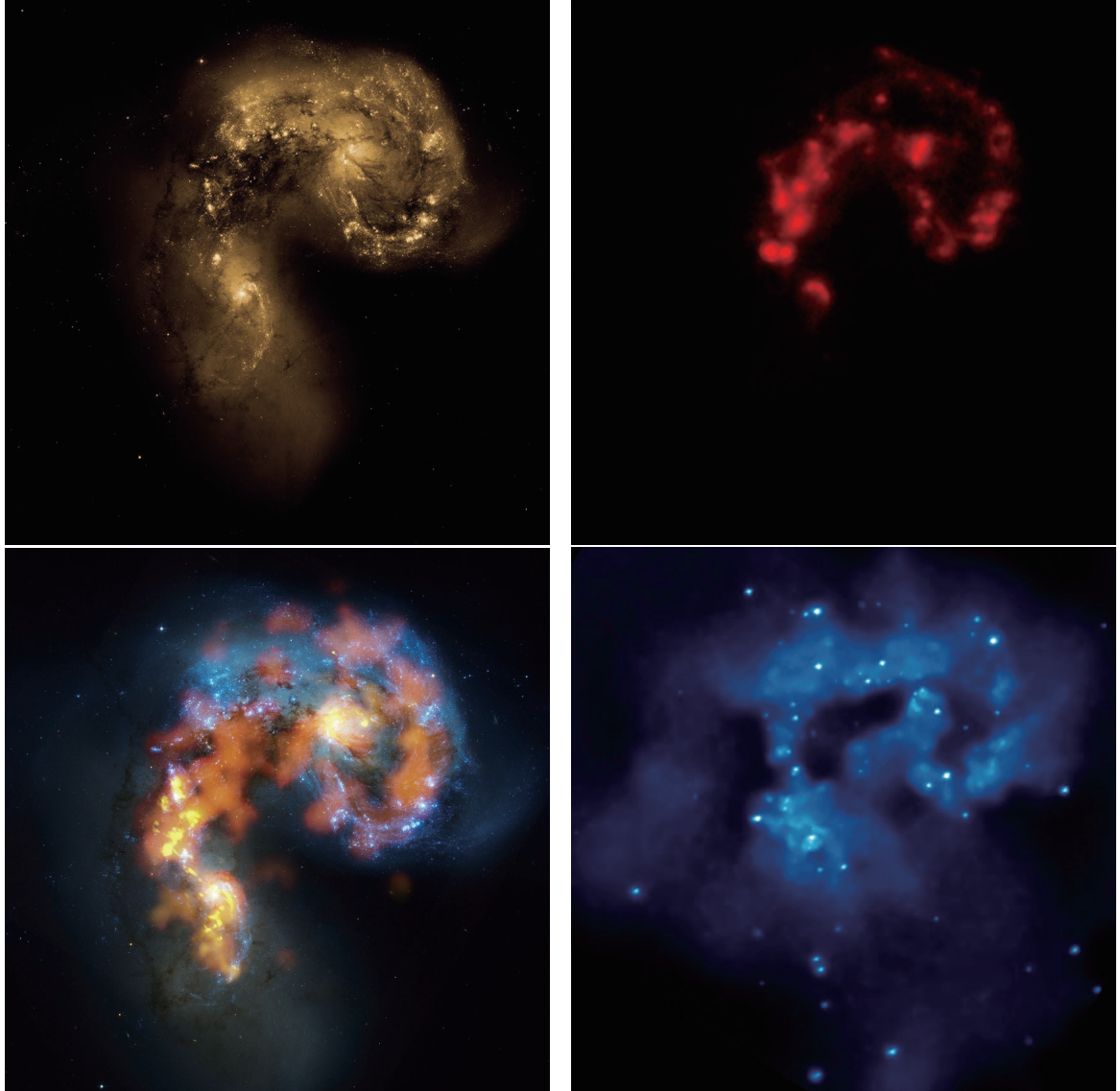


Figure 1.1: An example of multi-wavelength observations: optical (upper-left), infrared (upper-right), radio (bottom-left), and, X-ray (bottom-right). The object is the Antennae galaxies. The radio image is a multi CO line image overlaid on the optical image.

Image credit—Optical: NASA/STScI, Infrared: NASA/JPL-Caltech, Radio: B. Saxton, (NRAO/AUI/NSF), ALMA (ESO/NAOJ/NRAO) (Background optical image: the NASA/ESA Hubble Space Telescope), X-ray: NASA/CXC/SAO/J.DePasquale.

galactic X-ray sources. In addition, diffuse X-ray emission traces the galactic feedback from AGNs as well as from stars in the form of stellar winds and supernovae.

Galaxies are fundamental components of the Universe, and thus investigating galaxies leads to understanding the Universe itself. Technical improvements of observational instruments enable us to observe galaxies at redshifts up to  $z \sim 7.5$  (Finkelstein et al., 2013). Sensitivity and spatial resolution of observations have been limited, however, so that we cannot directly investigate the evolutionary history of distant galaxies. Thus, as a first step, it is important to study nearby galaxies in detail, which might provide clues to an understanding of distant galaxies in the early Universe.

## 1.2 Galaxy Classification

The classification of galaxies is a fundamental tool in astronomy. A classification scheme usually provides new insight into extragalactic astronomy and allows us to build a deep understanding of how galaxies form and evolve. Thus classification schemes have been developed for specific purposes.

### 1.2.1 Morphological Classification

Galaxies have been historically classified according to their apparent morphology. The most famous morphological classification is the Hubble’s “tuning fork” scheme (Hubble, 1958, Figure 1.2). Galaxies with different morphologies have evolved in different ways. Therefore morphological classification usually turns out to correlate with a difference in physical properties of galaxies. We provide a brief introduction about four main types of galaxies.

- **Elliptical galaxies** ( $En$ ) have nearly elliptical isophotes without any clearly defined structure. The surface brightness profiles of elliptical galaxies are well fit by Sérsic profile (see § 2.1). They are subdivided according to their ellipticity  $\epsilon \equiv (1 - b/a)$  ( $0 \leq \epsilon \lesssim 0.7$ ), where  $a$  and  $b$  are the semimajor and semiminor axes, respectively. The notation  $En$  is used to classify ellipticals with respect to the ellipticity ( $n = 10\epsilon$  (integer value)). They are composed of old, low-mass stars and little interstellar matter, which results in low rates of star formation. The motion of stars is predominantly random motion. Elliptical galaxies are preferentially found close to the centers of galaxy clusters. Elliptical galaxies are called “**early-type**” galaxies. This name does not imply any interpretation but exists only for historical reasons.

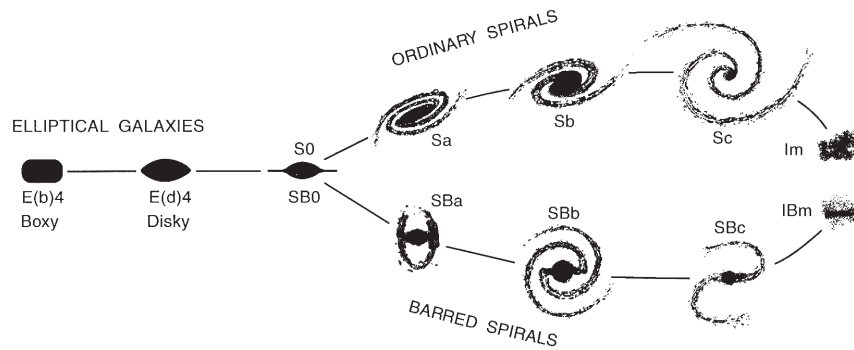


Figure 1.2: Hubble's tuning fork for galaxy classification.

Image credit—Kormendy & Bender (1996) (reproduced by permission of the AAS.)

- **S0 galaxies (lenticular galaxies)** (S0) are intermediates between ellipticals and spirals in the classification scheme. They consist of a bulge and a large enveloping region, which appears like a disk without spiral arms. They are subdivided into S0 and SB0, depending on whether or not they show a bar. S0 galaxies have used up or lost most of the interstellar matter and thus have little ongoing star formation. S0 galaxies and elliptical galaxies share common properties such as spectral features and scaling relations, and they are referred to as **early-type galaxies**.
- **Spiral galaxies** ( $Sx$ ) contain a rotating disk with spiral arms and a central bulge. These structures are surrounded by a much fainter halo of stars, many of which are part of globular clusters. They are divided into two subclasses: ordinary spirals ( $Sx$ ) and barred spirals ( $SBx$ ). In each of these subclasses, they are further divided according to the bulge-to-disk brightness ratio, and the notation  $Sx$  presents the brightness ratio ( $x = a/b/c$ ). Spiral arms are sites of ongoing star formation and young, hot OB stars inhabit them. The motion of stars is dominated by rotation in a disk, while it is predominantly random motion in a bulge. Spiral galaxies are mostly found in low-density regions and are rare in the centers of galaxy clusters. They are also called "**late-type**" galaxies. This name is only historical as well as early-type galaxies.
- **Irregular galaxies** (Irr) are galaxies with only weak (Irr I) or no (Irr II) regular structure. Irregular galaxies usually contain abundant amounts of gas and dust. Some of them were once spiral or elliptical galaxies, but they were deformed by gravitational interaction with neighbors. The classification between two subtypes (Irr I and Irr II) is often refined. In particular, the sequence of spirals is extended to the classes of irregular galaxies (e.g., Sdm, Sm, Im, IBm).

### 1.2.2 Starburst Galaxies

The light from “normal” galaxies (ellipticals and spirals) is emitted mainly by stars. Therefore, in principle, the spectral energy distribution of normal galaxies is a composite of the spectra of their stellar population. In contrast, another type of galaxy, the so-called **starburst galaxy**, has a spectral energy distribution dominated by thermal dust emission at far-infrared (FIR) and submillimeter wavelengths or by radiation from young massive stars in the blue (optical) and UV regions. Starburst galaxies are characterized by strongly enhanced star formation. The star formation rate (SFR) can be larger than normal galaxies by a factor of  $10^{2-3}$  ( $\text{SFR} \gtrsim 100 M_{\odot} \text{ yr}^{-1}$ ; see also Kennicutt, 1998), whereas the Milky Way, which is a typical normal galaxy, forms star with rate of a few  $M_{\odot} \text{ yr}^{-1}$  (e.g., Murray & Rahman, 2010). The SFR in starburst galaxies is so large that these galaxies will consume their gas reservoir, from which stars are newly forming, on a short timescale after which the SFR will decrease. Thus, starburst phase is a brief period of galaxy evolution. The primary cause of starbursts is gravitational interaction between galaxies. The majority of starburst galaxies appears to be in the midst of a merger or a close encounter with other galaxies. An impressive example of starburst galaxies is an intermediate-stage merger known as the Antennae galaxies (see Figure 1.1).

### 1.2.3 Ultra/Luminous Infrared Galaxies

**Luminous infrared galaxies (LIRGs)** are galaxies with FIR luminosities  $L_{\text{FIR}}$  above  $10^{11} L_{\odot}$ , and galaxies with  $L_{\text{FIR}} \geq 10^{12} L_{\odot}$  are especially called **ultraluminous infrared galaxies (ULIRGs)** (Sanders & Mirabel, 1996). Many LIRGs and ULIRGs were discovered in 1984 by the *IRAS* satellite (Neugebauer et al., 1984). The bulk of the IR luminosity for U/LIRGs comes from dust heating due to intense starbursts within giant molecular clouds. If star formation takes place in the interior of dense molecular clouds, which contain large amounts of dust, strong radiation from young luminous stars heats the surrounding dust and the dust reemits it at infrared wavelengths. In some cases, the IR luminosity of U/LIRGs comes from an **active galactic nucleus (AGN)**, which shows significant emission in all wavelengths from a compact region at the centre of a galaxy. The majority of U/LIRGs appears to be during a process of a merger and shows strongly disrupted morphology. Therefore, U/LIRGs are closely related to gravitational interactions between galaxies (e.g., Arp 220 and NGC 6240). In addition, ULIRGs may represent an important stage in the formation of quasars and powerful radio galaxies (see also Sanders & Mirabel, 1996).

## 1.3 Galaxy Mergers

### 1.3.1 Overview

Galaxy Mergers are galaxies in the process of colliding or merging with other galaxies. Mergers are also called interacting galaxies or merging galaxies. Galaxy interactions and mergers play an important role in the formation and evolution of galaxies, as illustrated by the increasing galaxy merger rate as one goes to higher redshift (Figure 1.3; Bundy et al., 2009; Bridge et al., 2010). Gravitational interactions between galaxies have powerful effects on their morphology and physical states. The degree of the effect depends on a wide variety of parameters such as collision orbit, collision speed, and relative size. Galaxy mergers are also known to enhance star formation activities as seen in the increasing fraction of tidally distorted morphologies. Therefore, galaxy mergers are closely related to galaxy formation and evolution.

Hubble (1936) noticed the existence of galaxies whose morphologies were quite unusual and later classified them as “highly peculiar objects” (Hubble, 1958). Arp (1966) compiled a catalog of 338 peculiar galaxies from the Palomar all sky survey (Minkowski & Abell, 1963). Similar cataloging projects were carried out by Vorontsov-Velyaminov (1959, 1977) and Arp & Madore (1987). Larson & Tinsley (1978) found early observational evidence that galaxies in the Arp catalog showed a higher level of star formation activity than the control sample of normal galaxies obtained from the Hubble atlas. This was confirmed by the *IRAS* satellite (Neugebauer et al., 1984). It discovered a new population of galaxies with high IR luminosities (U/LIRGs, see § 1.2.3), many of which showed highly disturbed morphology, indicating recent or past galaxy interactions.

Numerical simulations have provided new insights into studies of galaxy mergers. The first analog n-body simulation of galaxy interaction was carried out by Holmberg (1941). He demonstrated that the degree of tidal disturbance depended on collision orbits. Toomre & Toomre (1972) proved using the restricted three-body approximation that tidal interaction could profoundly alter the distribution and dynamics of stars in a relatively short time. In addition, they predicted that major mergers would result in elliptical galaxies and that star formation activity was enhanced by galaxy interaction, fueling gas to nuclear regions. These predictions were later confirmed by large scale numerical simulations (e.g., Barnes & Hernquist, 1992; Mihos & Hernquist, 1996; Springel et al., 2005).

There are a number of excellent reviews and papers on galaxy mergers: Schweizer (1983, 1986, 1990), Barnes & Hernquist (1992), Struck (1999), and Hopkins et al. (2009, § 1).

### 1.3.2 Merger Classification

Galaxy mergers are classified into distinct groups according to their properties.

- **Major/Minor mergers:** Mergers are classified into two types by the mass ratio of their progenitors. One type is major mergers with mass ratios in the range 1:1–3:1 (or 1:1–4:1), and the other is minor mergers with mass ratios below 3:1 (or 4:1). Major mergers, which can lead to significant dynamical and morphological disturbances, are strongly linked to starbursts and AGNs (e.g., Sanders & Mirabel, 1996). Minor mergers including small satellite-galaxy interactions are thought to occur more frequently than major mergers (e.g., Jogee et al., 2009).
- **Wet/Dry mergers:** Mergers are classified into two types by their gas richness. Wet mergers are gas-rich mergers which may produce a larger amount of star formation and trigger starburst, AGN and quasar activities (e.g., Hopkins et al., 2006). On the other hand, dry mergers are gas-poor mergers, most of which are formed by mergers between gas-poor early-type galaxies. These mergers may not involve dramatic changes in the star formation rate but can play an important role in the stellar mass growth (e.g., Naab et al., 2006; Lin et al., 2008).

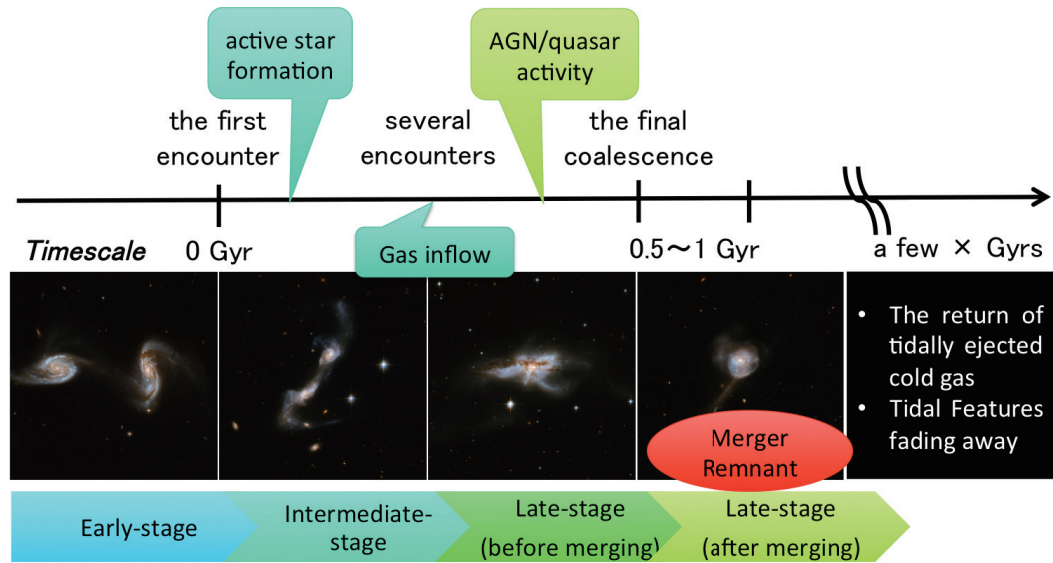


Figure 1.4: Merger sequence and timescale. A merger sequence of major mergers is divided into three stages: early-, intermediate-, and late-stage. A typical timescale of galaxy merge from the first encounter to the final coalescence is 1 Gyr, and a timescale of returning of tidally ejected material after the coalescence is estimated to extend over many Gyr.

Image credit—NASA, ESA, the Hubble Heritage (STScI/AURA)-ESA/Hubble Collaboration, and A. Evans (University of Virginia, Charlottesville/NRAO/Stony Brook University)

### 1.3.3 Merger Sequence and Timescale

Toomre (1977) first demonstrated that major mergers can be sequenced the so-called “Toomre Sequence”. He compiled a set of 11 apparently interacting and merging galaxies from available optical images, and roughly ordered them according to the completeness of the interaction based purely on their optical morphology. The sequence of major mergers is usually divided into three stages: early-stage, intermediate-stage, and late-stage (Figure 1.4), but there is no strict definition to each stage. The typical timescale of galaxy merging from the first encounter to the final coalescence is 1 Gyr (Springel & Hernquist, 2005; Chien & Barnes, 2010), and the timescale of the returning of tidally ejected material after the coalescence is estimated to extend over many Gyr (Hibbard & Mihos, 1995), which is longer compared to the timescale from the first encounter to the final coalescence. General characteristics observed and expected from numerical simulations in each stage are below.

- **Early-stage mergers** (before the first encounter): Galaxies approach each other but are still distinct. The morphology starts to be distorted, and an optical bridge connects the galaxies.

- **Intermediate-stage mergers** (after the first encounter): The apparent morphology is strongly distorted, and tidal tails are formed. Gas inflows into the nuclei, triggering starbursts.
- **Late-stage mergers** (during merger and after merging): AGN and quasar activities are often observed in late-stage mergers, where a growth of a supermassive black hole is also expected. After merging, the system represents a single stellar body and will relax to a normal galaxy.

## 1.4 Galaxy Formation and Evolution

### 1.4.1 Galaxy Formation in the $\Lambda$ -CDM model

The Cosmic Microwave Background (CMB) was discovered by Penzias & Wilson (1965), which was confirmed as the first observational evidence of the Big Bang by Dicke et al. (1965). Since the discovery of the CMB, a number of ground-based observations have been carried out to search for small anisotropies in the CMB, which are seeds of structures in the present Universe. The structures evolved out of very small density fluctuations in the early Universe. Thus these density fluctuations should be visible as small temperature fluctuations in the CMB. The NASA Cosmic Background Explorer (COBE) satellite finally confirmed temperature fluctuations in the CMB map (Smoot et al., 1992), and the  $\Lambda$ -CDM cosmological model came under consideration.

The  $\Lambda$ -CDM model is a cosmological model with the cosmological constant ( $\Lambda$ ) and cold dark matter (CDM).  $\Lambda$  is the energy density in a vacuum that explains the accelerating expansion of the Universe. It is currently thought to be associated with dark energy, which constitutes about 70% of the energy density of the present Universe. CDM is necessary to account for gravitational effects observed in large-scale structures, including the rotation of galaxies and the gravitational lensing of light by galaxy clusters. These gravitational effects cannot be explained by the quantity of observable matter. The dark matter component is estimated to constitute about 25% of the mass energy density of the Universe. The remaining 5% is comprised of all baryonic matter observed as atoms and chemical elements. The  $\Lambda$ -CDM model is today referred to as the standard cosmological model, which is able to account for nearly all the large-scale features of the observable Universe, including the accelerating expansion of the Universe and the large-scale structure in the distribution of galaxies.

In the  $\Lambda$ -CDM cosmological model, structure formation in the Universe basically proceeds hierarchically. Small gravitationally bound structures such as stars and stellar clusters form first, and



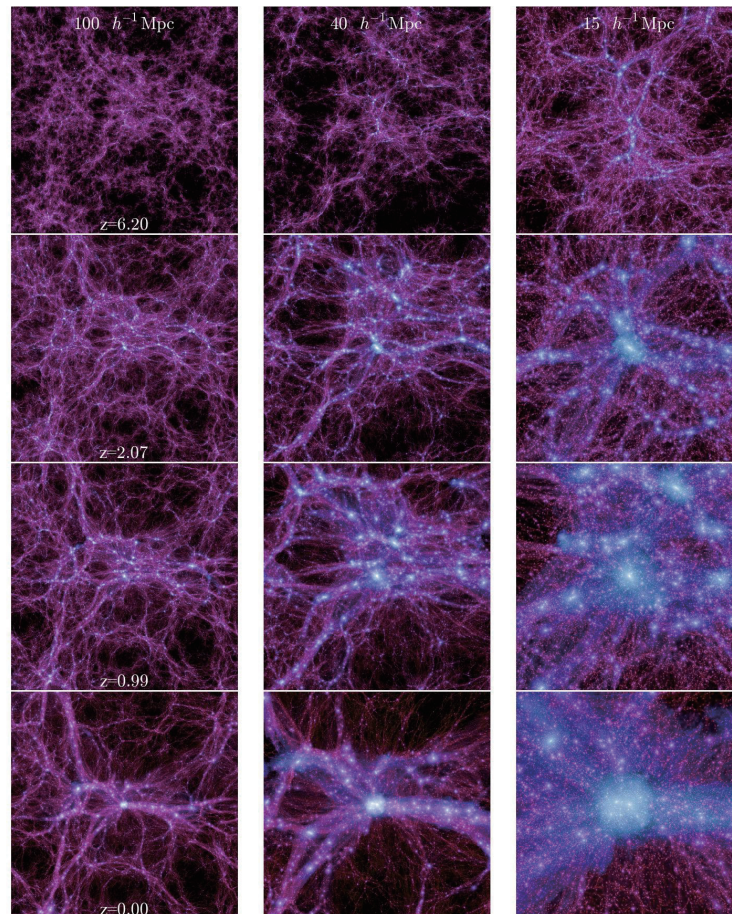


Figure 1.5: Time evolution of the formation of the most massive dark-matter halo in the Millennium-II Simulation (Boylan-Kolchin et al., 2009). The halo is shown at three comoving scales (from left to right:  $100$ ,  $40$  and  $1 \text{ Mpc}^{-1}$ ) and at four different cosmological epochs (from top to bottom:  $z = 6.2$ ,  $2.07$ ,  $0.99$  and  $0$ ).

Image credit—Boylan-Kolchin et al. (2009) (reproduced by permission of the AAS.)

subsequently they merge to form massive gravitationally bound systems such as galaxies, followed by groups, clusters, and superclusters of galaxies. In other words, low-mass dark matter halos form first and subsequently more massive halos form by merging of lower-mass halos (Figure 1.5; Boylan-Kolchin et al., 2009). Gas in a halo cools efficiently and then it is converted into stars. Gas initially accumulates in a disk and subsequently will form stellar disk when the density of the gas in the disk reaches a threshold for star formation. It is now understood that disk galaxies are formed in this way. However, disk galaxies can lose angular momentum during the process of galaxy collision. It is not understood whether disk galaxies will survive after galaxy collision. In contrast, it has been long predicted that the primary mechanism of the formation of early-type galaxies is major mergers (Toomre & Toomre, 1972; Barnes & Hernquist, 1992). Early-type galaxies are often found in the centers of galaxy clusters, where merging is expected to be frequent due to a high galaxy-density. In addition, observations using absorption-line indicate that a significant fraction of early-type galaxies in galaxy clusters has undergone recent star formation (Barger et al., 1996). This bottom-up formation scenario of early-type galaxies is naturally expected for structure formation processes in the  $\Lambda$ -CDM cosmological model.

### 1.4.2 Galaxy Evolution through Galaxy Mergers

In the  $\Lambda$ -CDM cosmological model, galaxy interactions and mergers are related to the formation and evolution of galaxies. Galaxies undergo several interactions and mergers during their lifetime, thus galaxies evolve by repeated galaxy merger events. Since the 1970's, it has been long predicted from numerical simulations that a major merger of two disk galaxies results in a formation of a spheroid-dominated early-type galaxy (e.g., Toomre, 1977; Barnes & Hernquist, 1992; Naab & Burkert, 2003). This classical scenario is supported by observations, revealing stellar structures of merger remnants (e.g., Schweizer, 1982; Rothberg & Joseph, 2006a) and signatures of mergers such as shells and tidal features around elliptical galaxies (e.g., Schweizer & Seitzer, 1992; Schweizer, 1996).

Contrary to the classical scenario of merger evolution, recent high-resolution simulations that include more realistic gas physics have shown that not all of the major mergers will become an early-type galaxy, but some will reemerge as a disk-dominated late-type galaxy (Barnes, 2002; Robertson & Bullock, 2008; Hopkins et al., 2009). Gas in mergers that do not lose significant angular momentum through stellar torque will survive the collision, reforming a gaseous (and subsequently a stellar) disk

(Figure 1.6; Springel & Hernquist, 2005), while gas that falls to the galaxy center will contribute to a nuclear starburst and subsequent formation of the spheroidal component. This merging process is a candidate for a formation scenario of cold molecular gas disks, that is otherwise not well understood. Another possibility is cosmological accretion (Kereš et al., 2005; Dekel et al., 2009) of low-angular momentum cold gas that eventually settles onto the galactic disk, but this scenario is predicted to be likely more relevant in the outskirts of the galaxies in the local Universe. In galaxy mergers, the chance of disk survival during the merging event depends on orbital parameters, mass ratio, and gas mass ratio of the progenitors (Hopkins et al., 2009), and the same simulations also suggest that increasing the gas mass fraction to the stellar mass leads to a more efficient disk survival (Figure 1.7) as there are fewer stars to lose angular momentum to. In case of pre-mergers with the gas mass fraction of 10 %, which is a typical value for late-type galaxies in the local Universe, the surviving disk fraction after merging is expected to be a few % as shown in Figure 1.7 (Hopkins et al., 2009). The new scenario of merger evolution might resolve a problem that the number of elliptical galaxies in the local Universe is much less than the theoretical value based on the classical scenario (Bournaud et al., 2007).

Minor mergers are thought to occur more frequently than major mergers. Numerical simulations have shown that minor mergers form late-type galaxies (Quinn et al., 1993; Walker et al., 1996) and hybrid systems with spiral-like morphology but elliptical-like kinematics (Bournaud et al., 2004). Such systems were observed by Jog & Chitre (2002). However other numerical simulations predict that late-type galaxies cannot have survived due to multiple minor mergers because repeated minor mergers destroy disks into spheroids (Bournaud et al., 2007), and compact high-redshift spheroids can evolve into local early-type galaxies in the process of minor mergers (Naab et al., 2009). The evolution of minor mergers is still under discussion as well as the evolution of major mergers.

## 1.5 Merger Remnants

**Merger remnants** are completely merged galaxies with a single nucleus, and still have tidal tails, shells, and loops, indicating dynamical interactions (e.g., Figure 1.4). Merger remnants are classified as late-stage mergers (see § 1.3.3), and will relax to normal galaxies over time (a few Gyr; Hibbard & Mihos, 1995), returning of tidally ejected material.

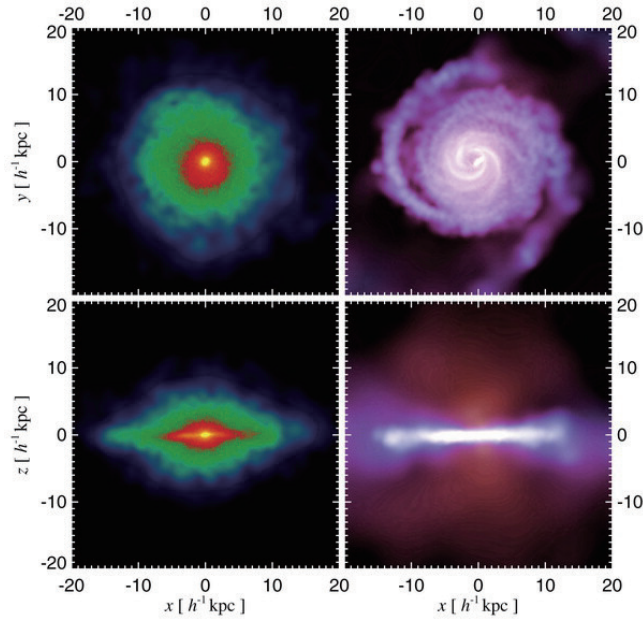


Figure 1.6: Result of a simulation of reformed extended gas disk (Springel & Hernquist, 2005), showing the distribution of stars (left) and gas (right) in a merger remnant in 1.96 Gyr from the first encounter. The top panels show a face-on view, and the bottom panels show an edge-on view.

Image credit—Springel & Hernquist (2005) (reproduced by permission of the AAS.)

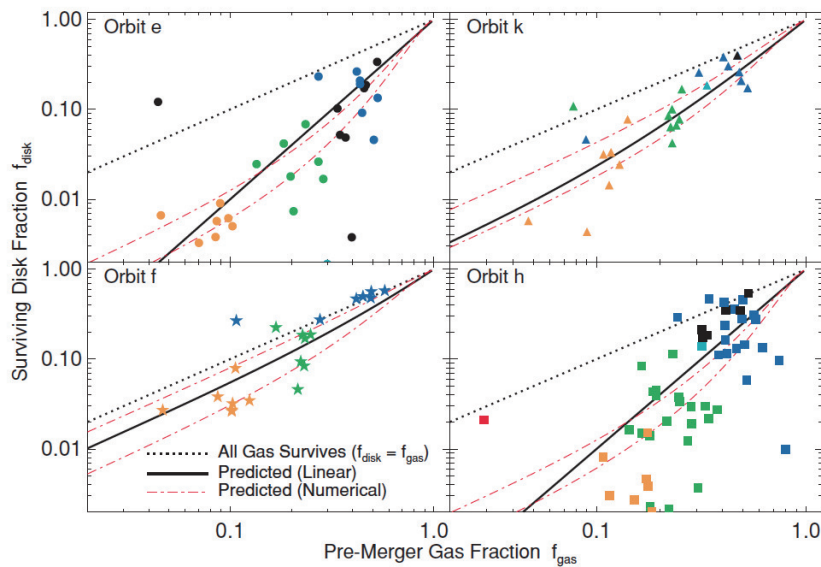


Figure 1.7: The surviving disk fraction as a fraction of gas mass fractions just before the final coalescence (pre-merger gas fraction), for 1:1 major mass-ratio mergers (Hopkins et al., 2009). The disk fraction increases with the gas mass fraction.

Image credit—Hopkins et al. (2009) (reproduced by permission of the AAS.)

### 1.5.1 Previous Studies on Merger Remnants

Most previous studies on merger remnants (e.g., Lake & Dressler, 1986; Shier & Fischer, 1998; James et al., 1999; Genzel et al., 2001; Dasyra et al., 2006; Rothberg & Joseph, 2004, 2006a,b) focused on the stellar properties. This is because the classical scenario, in which a major merger between two disk galaxies forms a new elliptical galaxy (see § 1.4.2), received higher attention. These studies show that the kinematic and photometric properties of the stellar components in merger remnants, including velocity dispersions, stellar masses and light profiles, are consistent with typical elliptical galaxies and have supported the classical hypothesis for the evolution of major mergers.

A large-scale observational study of the large sample of merger remnants in the local Universe was carried out by Rothberg & Joseph. They present  $K$ -band photometry for 51 candidate of merger remnants (Rothberg & Joseph, 2004). Using both the de Vaucouleurs profile and the Sérsic profile, they find that the stellar components in a majority of the sample sources have undergone violent relaxation, though seven sources show evidence for incomplete phase mixing. Their analysis also indicates the presence of “excess light” in the surface brightness profiles of nearly one-third of the sample, suggesting the effect of starbursts induced by the dissipative collapse of the gas. Two years later, they conducted a spectroscopic study for a subsample of 38 merger remnants (Rothberg & Joseph, 2006a,b) to investigate whether the merger remnants have the same stellar properties as elliptical galaxies, such as stellar luminosity and distribution, central stellar velocity dispersion, and metallicity. As a result, the merger remnants show a strong correlation among the parameters of the fundamental plane, which is embedded in a three-dimensional space comprised of the central velocity dispersion, the effective radius, and the surface brightness within the effective radius (Djorgovski & Davis, 1987). Bulges in spiral galaxies and elliptical galaxies share the fundamental plane (e.g., Bender et al., 1992). In addition, their analysis shows that 11 % of the subsample is boxy and anisotropically supported, while 47 % is disky and rotationally supported. The merger remnants show variation in shape and rotation. This may provide an observational diagnostic for discriminating among evolution scenario of merger remnants.

Observational studies of molecular gas in merger remnants have been conducted (e.g., Downes & Solomon, 1998; Wilson et al., 2008), but most of the previous samples are mergers with high FIR luminosities (U/LIRGs). In addition, these studies focused on the the physical state of molecular gas. There are few studies focusing on the morphology of molecular gas.

### 1.5.2 The Evolution of Merger Remnants

Although the main bodies of merger remnants become devoid of distinct structure, they show plumes and shells in the outer regions after merging (e.g., Rothberg & Joseph, 2004). These features are smoothed out over time. However, returning of tidal material can lengthen the completion of the phase-mixing process. The most tightly bound gaseous material returns to the main body rather quickly and can resettle into a warped disk (Mihos & Hernquist, 1996; Naab & Burkert, 2001; Barnes, 2002). Such a warped gaseous disk has been observed in the nearby merger remnant Centaurus A (Nicholson et al., 1992). In contrast, the loosely bound, high-angular momentum gas falls back to ever-increasing radii over longer time scales, forming a more extended disk outside several effective radii in the merger remnant. The timescale of returning of tidally ejected material is estimated to extend over many Gyr (Hibbard & Mihos, 1995), which is longer compared to the timescale from the first encounter to the final coalescence ( $10^{8-9}$  yr; Hibbard & Mihos, 1995; Chien & Barnes, 2010). Therefore, the process of phase mixing takes much longer to complete than violent relaxation.

As mentioned in the previous section (§ 1.4.2), early numerical simulations of galaxy mergers (e.g., Barnes & Hernquist, 1992) demonstrated that a major merger of two disk galaxies can produce an object with an  $r^{1/4}$  stellar distribution like typical elliptical galaxies. However, in recent simulations with a gaseous component, disky and rotationally supported merger remnants also form from major mergers (e.g., Springel & Hernquist, 2005). This raises several questions: Do merger remnants with an extended gas disk really exist? and will they evolve into elliptical galaxies with properties similar to those in present-day elliptical galaxies, or into a different type of galaxy? In order to answer these questions, observational studies focusing on a gaseous component in merger remnants are required along with further advanced numerical simulations.

## 1.6 Radio Astronomy and Interferometry

Radio astronomy is the study of objects in the Universe by analyzing the radio waves emitted from the objects. The very first observations go back to Karl Jansky's discovery in the 1930's. He observed radiation from the Milky Way using a rotating radio antenna. Tow decades later, in 1951, Ewen and Purcell discovered the 21 cm hydrogen line from the Milky Way using a horn antenna. Subsequent observations have provided a whole new outlook on already known objects such as stars and galaxies, while revealing new types of objects, such as radio galaxies, quasars, pulsars, and masers.

### 1.6.1 Radio Observations in the CO line

The most abundant molecule in the Universe is molecular hydrogen ( $\text{H}_2$ ), which is a symmetric homo-nuclear molecule with no permanent electric dipole moment, hence we cannot observe the  $\text{H}_2$  line at radio wavelengths because it does not have a permitted transition. The second most abundant molecule is carbon monoxide ( $^{12}\text{CO}$ ; hereafter CO), which has been used extensively as an indirect tracer of  $\text{H}_2$  despite its low relative abundance ( $N_{\text{CO}}/N_{\text{H}_2} = 10^{-4} - 10^{-5}$ ; Tielens, 2005). Collisions between CO and  $\text{H}_2$  excite the CO to higher rotational states (to  $J = 2, 3, \dots$ ), which subsequently returns to the lower energy level by radiating the excess energy away. Because CO has a low dipole moment, it is easily excited to higher  $J$  levels at a low critical density ( $n_{\text{crit}} = 1.1 \times 10^3 \text{ cm}^{-3}$  for CO (1–0); Tielens, 2005) and an upper energy level ( $E_{\text{u}} = 5.5 \text{ K}$  for CO (1–0); Tielens, 2005).

The lowest  $J$  transition of CO, CO (1–0) line, is the best tracer of the diffuse extended disk and of the kinematics of the cold molecular gas. On the other hand, a high  $J$  transition of CO is a good tracers of denser and warmer molecular gas related directly to star formation, because the critical density and the upper energy level are higher than those of the CO (1–0).

In general, the CO (1-0) line is optically thick, which satisfies the optical depth  $\tau_{\nu} > 1$ . An optically thick line is one in which the average photon of frequency  $\nu$  cannot traverse the entire medium without being absorbed. Thus we observe radiation emitted from the surface of molecular clouds rather than from the core of molecular clouds. In contrast, an optically thin line is less affected by absorption and thus we can investigate the core of molecular clouds using optically thin lines.

### 1.6.2 Radio Interferometer

Radio astronomy is conducted using radio antennas (telescopes), that are either used singularly or used with multiple linked antennas utilizing the techniques of radio interferometry and aperture synthesis. The former is a single-dish telescope and the latter is a radio interferometer. Radio interferometers achieve higher angular resolution than single-dish telescopes because the angular resolution  $\theta$  is determined by approximately  $\lambda/D$ , where  $\lambda$  is the wavelength observed and  $D$  is the diameter of the single-dish telescope or the longest baseline length. Though early interferometers were used as a single baseline between two antennas for measurement, later interferometers, such as the Very Large Array (VLA), form arrays of telescopes arranged in a pattern on the ground. A limited number of baselines will result in insufficient  $uv$ -plane coverage and low-quality imaging.

There are currently-operated millimeter/submillimeter interferometers in the world (Figure 1.8):

- **Atacama Large Millimeter/submillimeter Array (ALMA)**

ALMA is the most powerful millimeter/submillimeter interferometer, which consists of up to 64 12-m antennas and a compact array (ACA;  $12 \times 7$ -m antennas +  $4 \times 12$ -m antennas). The proposed maximum baseline is 18.5 km, which provides  $0''.03$  angular resolution at 115 GHz. It is built in the Atacama Desert of northern Chile at an altitude of approximately 5000 m. Incoming radio waves are less susceptible to absorption by terrestrial water vapor in the ALMA site and thus we can observe radio waves at relatively shorter wavelengths (at higher frequencies).

- **Combined Array for Research in Millimeter-wave Astronomy (CARMA)**

The CARMA is a millimeter-wave interferometer, which combines the previously independent Owens Valley Millimeter Observatory (OVRO) array and Berkeley-Illinois-Maryland Association (BIMA) array. The number of antennas is increased to 23 ( $6 \times 10.4$  m antennas +  $9 \times 6.1$  m antennas +  $8 \times 3.5$  m antennas), providing a substantial improvement in  $uv$  coverage. It is located at a high-altitude site ( $\sim 2200$  m) in the Inyo Mountains of California, USA. The maximum baseline is approximately 2 km, which provides  $\sim 0''.3$  angular resolution at 115 GHz.

- **Plateau de Bure Interferometer (PdBI)**

The PdBI is one of the most sensitive millimeter interferometers, operated by the Institut de radioastronomie millimétrique (IRAM). It is situated on the Plateau de Bure at altitude of 2550 m in the French Alps. During its history, the PdBI underwent several track extensions and received additional antennas and technical upgrades. The interferometer now consists of six 15 m antennas with powerful dual-polarisation receivers for the 3mm and 1mm observing bands. The maximum baseline is 760 m, which provides  $0''.7$  angular resolution at 115 GHz.

- **Submillimeter Array (SMA)**

The SMA is the only submillimeter-wave interferometer in the north hemisphere, operated at wide-range frequencies from 180 GHz to 700 GHz. It consists of eight 6 m antennas located at an altitude of 4100 m on Mauna Kea in Hawaii, USA. The digital correlators allows flexible allocation of thousands of spectral channels. The maximum baseline is 509 m, which provides  $\sim 0''.4$  angular resolution at 345 GHz. It can be operated together with the James Clerk Maxwell Telescope (JCMT) and the Caltech Submillimeter Observatory (CSO) as eSMA.





Figure 1.8: Existing millimeter/submillimeter interferometers: ALMA (upper-left), CARMA (upper-right; ©CARMA), PdBI (bottom-left; ©IRAM), and SMA (bottom-right)

## 1.7 Scientific Goals and Thesis Structure

In this thesis, I statically reveal the distribution and kinematics of the molecular gas in late-stage mergers, using our own and archival observational data, which is the largest interferometric CO survey on merging galaxies to date. This is the first step in our series of studies which emphasize the cold molecular gas in merger remnants, instead of the stellar component which has been the focus of previous studies. From this new compilation of high quality CO data, I give new insights into the evolution of galaxies via galaxy mergers. This thesis opens up the possibility of additional future studies, for example comparative studies with numerical simulations, observations of the diffuse gas traced in HI, and dense gas traced in HCO<sup>+</sup>/HCN. Initial preparation is already underway and understanding the evolution of a major merger is our ultimate scientific goal.

The key scientific goal of this thesis involves understanding the properties of molecular gas in merger remnants. We have conducted a CO survey toward 27 optically-selected merger remnants in the local Universe using millimeter/submillimeter interferometers (ALMA, SMA, and CARMA). Combined with archival data, we analyze the molecular gas in 37 optically-selected merger remnants in order to investigate the following main questions.

- **What is the distribution and kinematics of cold molecular gas in merger remnants?**

**(Chapter 2, and Chapter 3)**

Chapter 2 presents the CO images of 37 optically-selected merger remnants obtained at ALMA, SMA, CARMA and PdBI. Our study is the first systematic CO imaging survey of merger remnants. The distribution and kinematics of molecular gas are presented for each source to investigate the properties of the molecular gas in merger remnants in Chapter 3 and Chapter 4.

- **Do extended cold molecular gas disks form in merger remnants, as predicted from recent numerical simulations? (Chapter 2 and Chapter 3)**

Recent numerical simulations with realistic gas physics have shown that some gas-rich major-mergers will reemerge as a disk dominated late-type galaxy, by reforming an extended cold molecular gas disk (and subsequently a stellar disk) or via survival of the progenitor disks. In order to verify this scenario and look for observational evidence of an extended molecular disk

forming in merger remnants, the presence of the molecular gas disk is confirmed using fitting and modeling programs in Chapter 3. Chapter 4 focuses on the size of the gas disk.

- **Are the properties of the molecular gas in merger remnants different from early-type and late-type galaxies? (Chapter 4)**

Comparing the properties of the molecular gas in early-type galaxies and late-type galaxies, leads to better understanding of the nature of merger remnants. Combining with IR images, we investigate whether the global properties such as gas mass fraction and star formation activity in merger remnants are different from those of early- or late-type galaxies or not.

- **What type of galaxies will merger remnants evolve into? (Chapter 4)**

It has been long predicted from numerical simulations that a major merger of two disk galaxies results in a formation of the spheroid-dominated early-type galaxy. In the final section of Chapter 5, the evolution of merger remnants is discussed observationally by comparing the sizes of the molecular gas disks and gas mass fractions to early-type and late-type galaxies in the field. Finally, the observational implications are compared with theoretical predictions.

- **What's next? (Chapter 5)**

Chapter 6 begins with a summary of this thesis including answers to the questions addressed here. It is then followed by further implication and plans to better understand galaxy merging and the evolution and formation of galaxies in the local Universe through galaxy mergers.



## Chapter 5

# Summary and Future Prospects

### 5.1 Summary

Galaxies is one of the primary components of our observable Universe, and thus revealing the evolution and formation of galaxies is one of the biggest frontiers in understanding our Universe. Since Edwin Hubble discovered LTGs in the first half of the 19th century, the formation mechanism of LTGs, which comprise more than half of all galaxies, has been studied in detail. After half a century of Hubble's discovery, recent numerical simulations have shown that LTGs can form through galaxy mergers. The observational confirmation of this scenario had yet to come.

We have conducted a CO imaging survey of merger remnants (MRs) in the local Universe using millimeter/submillimeter interferometers including ALMA, SMA, and CARMA, and the NRO 45 m single-dish telescope in order to understand the properties of molecular gas and to investigate the evolution of MRs. This study is based on the largest systematic CO imaging survey of MRs to date, enabling, for the first time, a statistical analysis of molecular gas at their final stage of coalescence.

We have revealed, observationally, that merging events in the local Universe are indeed the cross-roads of galaxy evolution, reprocessing the otherwise slowly evolving galaxies into a mixture of types including ETGs and LTGs. This result has enormous significance in understanding the evolution of galaxies via galaxy mergers. Furthermore, this study opens up the door to additional studies, for example comparative studies with numerical simulations, and observations of the diffuse gas to confirm the returning of the ejected cold gas via tidal tails and cold gas stream/accretion. Future studies should also be targeted toward high- $z$  galaxies to understand the history of galaxy formation.

This thesis started out by addressing five main questions, each of which were investigated in detail in Chapters 2 – 4. Main conclusions are as follows:

- **What is the distribution and kinematics of cold molecular gas in merger remnants?**

We investigate interferometric CO maps of 37 optically-selected MRs, including seven sources which were undetected in the CO line. Twenty seven of these galaxies were newly obtained, and 10 are archival data. By fitting the CO velocity field with circular motion, we find that 65 % (24/37) of the sample show kinematical signatures of a rotating molecular gas disk. The sizes of these disks vary significantly from 1.1 kpc to 9.3 kpc. We also find that the emission peaks are clearly shifted from the galactic centers in 75 % (18/24) of the sources with gas disks, suggesting the presence of a ring and/or a bar. We were unable to fit the CO velocity field of other six sources with circular motion. These sources show clumpy distribution and complex velocity fields, indicating that the molecular gas is still strongly disturbed and has not settled in the galactic plane.

- **Are extended cold molecular gas disks formed in merger remnants, as predicted from recent numerical simulations?**

We compare the size of the molecular gas disk to the stellar spheroidal component for 24 MRs with CO detection. The size ratios ( $R_{\text{eff}}$ ) of the gas disk to the stellar component for 54 % (13/24) of the MRs are less than unity. Six MRs which are bright at infrared wavelengths have compact molecular gas disks, which may have formed by past gas inflow that was triggered by dynamical instability following the merging. On the other hand, **46 % (11/24) of the MRs have gas disks which are extended relative to the stellar component.** We also discover a possible positive correlation between  $R_{\text{ratio}}$  and the total far-infrared luminosity. This suggests that the physical activities that are responsible for increasing luminosity, namely starburst/AGN, are related to the formation of the extended molecular gas disks. The molecular gas disks in the MRs show various properties, and we conclude that our sample includes MRs at different stages of their evolution, progenitors of galaxies with different characteristics, or different initial conditions.

- **Are the properties of the molecular gas in merger remnants different from early-type and late-type galaxies?**

The size of the molecular gas disks in MRs is similar to those in the ETGs rather than LTGs. The ratio of molecular gas mass to stellar mass, the gas mass fraction, is found to be in the range 1 – 10 % for MRs. The gas mass fractions of the LTGs are distributed around 10 %, whereas the gas mass fractions of the ETGs are distributed over a wide range between 0.1 % and 10 %. A Kolmogorov-Smirnov test suggests that the distribution of the gas mass fractions are different among the three samples. When the gas mass fractions of ETG/LTGs are combined, however, the MRs are not significantly different. These statistics are not inconsistent with the possibility that the MRs include progenitors of both ETGs and LTGs. In a diagram plotting  $R_{\text{ratio}}$  versus the gas mass fraction, the distribution of MRs does not overlap with either the ETG or the LTG population. In short, **the molecular gas in MRs is on average similar to ETGs in terms of its disk size, but the MRs are in fact a distinct population with respect to their relation between size and mass relative to the stellar component.**

- **What type of galaxies do merger remnants evolve into?**

From comparisons of the MRs with ETGs and LTGs regarding their molecular gas and stellar components, **overall, our conclusion is that 65 % of the MRs evolve into ETGs, 5 % into LTGs, 14 % into either ETG/LTGs, and 16 % into galaxies which cannot be classified into ETG/LTGs.** Among the sources with observational signatures of molecular gas disks, we conclude that sources with a compact molecular gas disk will become ETGs regardless of the gas mass fraction, mainly because of the short depletion time of the molecular gas ( $\sim 10^8$  yr), and high gas concentration in the nuclear region. On the other hand, we find that sources with an extended molecular gas disk and a large gas mass fraction are likely to result in LTGs, unless there are further mechanisms which transport the molecular gas toward the central region (e.g., nuclear bar) thereby decreasing the disk size. Confirming the evolution path of the sources with an extended molecular gas disk and a low gas mass fraction requires further studies to investigate whether a large amount of cold gas will settle on the extended gas disks by the returning of the ejected cold gas via tidal tails and cold gas accretion. For six MRs whose velocity fields cannot be modeled with circular rotation, their clumpy morphology and complex gas structure

are not seen in either ETG/LTGs. The seven MRs which were not detected in CO will evolve into ETGs earlier than the MRs with the molecular gas disks. This study confirms, observationally, a new scenario that merging events are the crossroads of galaxy evolution, reprocessing them into a mixture of types including ETGs and LTGs.

Finally, we suggest two possibilities. One possibility is that returning the ejected cold gas via tidal tail might be a key to determine the evolution of MRs. The other is that large scale gas inflow is not the only scenario for the triggering of AGN/starburst activity, revealed by the presence of a population of MR with an extended molecular gas disk and AGN/starburst existing together.

## 5.2 Future Prospects: What's next?

This study is the first step in our series of studies which emphasize the cold molecular gas in MRs, instead of the stellar component which has been the focus of previous studies. We find new insights into the evolution of galaxies via galaxy mergers. There are remaining questions, and additional studies are necessary to completely understand the indications of this thesis study.

- **Where is the location of the star forming region in the extended molecular gas disk?**

We find clearly extended molecular gas disks in the MRs, while the reformation of an extended disk is a prediction of recent merger simulations. However, we do not know whether the stellar disks will be formed subsequently from the gas disks. In order to answer this question, we need to know where the star forming regions are located. Are the star forming regions located in the nucleus, throughout the extended disk, or both? To investigate this, we need to image the MRs in dense gas, using HCN/HCO<sup>+</sup> or a higher  $J$  transition of CO to compare to the low  $J$  emission, i.e., the CO (1–0) line. We will identify where warm and dense gas is distributed in the molecular disk, in other words, regions directly related to star formation. It is important to obtain both the diffuse gas and dense gas for investigating the spatial variation in the excitation or physical conditions as was demonstrated by us using the SMA data of the intermediate-stage merger Antennae galaxies (Ueda et al., 2012). Alternatively, we need new data of star forming tracers in optical/NIR. High-quality optical/NIR imaging can provide the



information of star forming region. Identifying star forming regions in extended molecular gas disk and revealing disk-dominated star formation can strengthen the scenario that mergers will evolve into disk-dominated disk galaxies.

- **Is it possible to expand the sizes of the gas disks by returning ejected cold gas?**

We find five MRs (Type A2) with extended molecular gas disks and low gas mass fractions. These galaxies either need to acquire gas mass in order to become comparable to LTGs, or decrease the size of its molecular disk to become comparable to ETGs. Confirming the evolution of these MRs, therefore, requires further studies to investigate whether a large amount of cold gas will settle on the extended gas disks by the returning of the ejected diffuse gas via tidal tails and cold gas stream/accretion. The neutral hydrogen (HI) gas is a good tracer of such gas.

The optically thin HI gas is one of the major components of the ISM in gas-rich galaxies. In our Galaxy, it constitutes about a half of the total gas mass of the ISM. The HI gas traces the loosely bound diffuse extended gas ( $n \sim 1 \text{ cm}^{-3}$ ) and is mainly distributed in the outskirts of the disk. Therefore the HI data allows us to examine the global structure of galaxies, including the properties at the outer regions where the density of the medium is too diffuse for molecular gas to exist. In addition, it is known that tidal interaction can strongly influence the HI distribution and kinematics (Yun et al., 1994), more so than the CO gas which is usually more centrally concentrated (Iono et al., 2004), and traces the higher density ( $> 10 \text{ cm}^{-3}$ ) regions.

Extended gas disks may form by the return of the tidally ejected material (Davis et al., 2011). We will search for kinematic signatures of large-scale infall of the tidally ejected HI gas and examine whether the HI and CO velocity fields share similar structures. If the MRs have HI disks, we will investigate whether the kinematical axis between the HI and CO disks are consistent. If the two alignments are consistent, this suggests the internal origin of the HI disk. On the other hand, if the kinematical axis are misaligned, the HI gas can be of external origin, i.e., infalling gas. We will also estimate the gas mass fraction including the atomic gas for the merger remnants. If kinematic signatures of infall are found, we will additionally investigate whether the infalling HI is massive enough to turn the galaxy into a typical LTG. If the gas mass fraction including the prospective HI is comparable to the gas mass fraction of LTGs, the MR may evolve into LTGs.



# Bibliography

- Aalto, S., Johansson, L. E. B., Booth, R. S., & Black, J. H. 1991, *A&A*, 249, 323
- Alatalo, K., Davis, T. A., Bureau, M., et al. 2013, *MNRAS*, 432, 1796
- Albrecht, M., Chini, R., Krügel, E., Müller, S. A. H., & Lemke, R. 2004, *A&A*, 414, 141
- Albrecht, M., Krügel, E., & Chini, R. 2007, *A&A*, 462, 575
- Alloin, D., & Dufloc, R. 1979, *A&A*, 78, L5
- Andreani, P., Casoli, F., & Gerin, M. 1995, *A&A*, 300, 43
- Annibali, F., Bressan, A., Rampazzo, R., Zeilinger, W. W., & Danese, L. 2007, *A&A*, 463, 455
- Armus, L., Charmandaris, V., Bernard-Salas, J., et al. 2007, *ApJ*, 656, 148
- Arp, H. 1966, *Atlas of peculiar galaxies* (Pasadena: California Inst. Technology, 1966)
- Arp, H. C., & Madore, B. 1987, *A catalogue of southern peculiar galaxies and associations* (Cambridge ; New York : Cambridge University Press, 1987.)
- Balick, B., Faber, S. M., & Gallagher, J. S. 1976, *ApJ*, 209, 710
- Barger, A. J., Aragon-Salamanca, A., Ellis, R. S., et al. 1996, *MNRAS*, 279, 1
- Barnes, J. E. 2002, *MNRAS*, 333, 481
- Barnes, J. E., & Hernquist, L. 1992, *ARA&A*, 30, 705
- Barnes, J. E., & Hernquist, L. E. 1991, *ApJ*, 370, L65

## BIBLIOGRAPHY

---

- Beichman, C. A., Neugebauer, G., Habing, H. J., Clegg, P. E., & Chester, T. J., eds. 1988, *Infrared astronomical satellite (IRAS) catalogs and atlases. Volume 1: Explanatory supplement, Vol. 1*
- Bender, R., Burstein, D., & Faber, S. M. 1992, *ApJ*, 399, 462
- Berentzen, I., Shlosman, I., Martinez-Valpuesta, I., & Heller, C. H. 2007, *ApJ*, 666, 189
- Bertram, T., Eckart, A., Krips, M., Staguhn, J. G., & Hackenberg, W. 2006, *A&A*, 448, 29
- Boquien, M., Duc, P.-A., Wu, Y., et al. 2009, *AJ*, 137, 4561
- Borne, K. D., & Richstone, D. O. 1991, *ApJ*, 369, 111
- Bottinelli, L., Gouguenheim, L., Fouque, P., & Paturel, G. 1990, *A&AS*, 82, 391
- Bottinelli, L., Durand, N., Fouque, P., et al. 1993, *A&AS*, 102, 57
- Bournaud, F., & Combes, F. 2002, *A&A*, 392, 83
- Bournaud, F., Combes, F., & Jog, C. J. 2004, *A&A*, 418, L27
- Bournaud, F., Jog, C. J., & Combes, F. 2007, *A&A*, 476, 1179
- Boylan-Kolchin, M., Springel, V., White, S. D. M., Jenkins, A., & Lemson, G. 2009, *MNRAS*, 398, 1150
- Brassington, N. J., Ponman, T. J., & Read, A. M. 2007, *MNRAS*, 377, 1439
- Bridge, C. R., Carlberg, R. G., & Sullivan, M. 2010, *ApJ*, 709, 1067
- Brightman, M., & Nandra, K. 2011, *MNRAS*, 414, 3084
- Brown, M. J. I., Jannuzi, B. T., Floyd, D. J. E., & Mould, J. R. 2011, *ApJ*, 731, L41
- Bundy, K., Fukugita, M., Ellis, R. S., et al. 2009, *ApJ*, 697, 1369
- Cappellari, M., Emsellem, E., Krajnović, D., et al. 2011, *MNRAS*, 413, 813
- Casoli, F., Dupraz, C., & Combes, F. 1992, *A&A*, 264, 55
- Chien, L.-H., & Barnes, J. E. 2010, *MNRAS*, 407, 43

- Chitre, A., & Jog, C. J. 2002, *A&A*, 388, 407
- Cicone, C., Maiolino, R., Sturm, E., et al. 2013, ArXiv e-prints, arXiv:1311.2595
- Condon, J. J., Anderson, M. L., & Helou, G. 1991, *ApJ*, 376, 95
- Condon, J. J., Cotton, W. D., & Broderick, J. J. 2002, *AJ*, 124, 675
- Condon, J. J., Cotton, W. D., Greisen, E. W., et al. 1998, *AJ*, 115, 1693
- Condon, J. J., Helou, G., Sanders, D. B., & Soifer, B. T. 1990, *ApJS*, 73, 359
- . 1996, *ApJS*, 103, 81
- Cox, A. L., & Sparke, L. S. 2004, *AJ*, 128, 2013
- Crabtree, D. R., & Smecker-Hane, T. 1994, in *Bulletin of the American Astronomical Society*, Vol. 26, American Astronomical Society Meeting Abstracts, #107.14
- Crocker, A. F., Bureau, M., Young, L. M., & Combes, F. 2011, *MNRAS*, 410, 1197
- Dasyra, K. M., Tacconi, L. J., Davies, R. I., et al. 2006, *ApJ*, 651, 835
- Davis, T. A., Alatalo, K., Sarzi, M., et al. 2011, *MNRAS*, 417, 882
- Davis, T. A., Alatalo, K., Bureau, M., et al. 2013, *MNRAS*, 429, 534
- Deeg, H.-J., Brinks, E., Duric, N., Klein, U., & Skillman, E. 1993, *ApJ*, 410, 626
- Dekel, A., Birnboim, Y., Engel, G., et al. 2009, *Nature*, 457, 451
- Denisiuk, E. K., Lipovetskii, V. A., & Afanasev, V. L. 1976, *Astrofizika*, 12, 665
- Deo, R. P., Crenshaw, D. M., Kraemer, S. B., et al. 2007, *ApJ*, 671, 124
- Dicke, R. H., Peebles, P. J. E., Roll, P. G., & Wilkinson, D. T. 1965, *ApJ*, 142, 414
- Djorgovski, S., & Davis, M. 1987, *ApJ*, 313, 59
- Downes, D., & Solomon, P. M. 1998, *ApJ*, 507, 615
- Epinat, B., Amram, P., Marcelin, M., et al. 2008, *MNRAS*, 388, 500

## BIBLIOGRAPHY

---

- Evans, A. S., Mazzarella, J. M., Surace, J. A., et al. 2005, *ApJS*, 159, 197
- Fernández, X., van Gorkom, J. H., Schweizer, F., & Barnes, J. E. 2010, *AJ*, 140, 1965
- Finkelstein, S. L., Papovich, C., Dickinson, M., et al. 2013, *ArXiv e-prints*, arXiv:1310.6031
- Fisher, D. B., Bolatto, A., Drory, N., et al. 2013, *ApJ*, 764, 174
- Fort, B. P., Prieur, J.-L., Carter, D., Meatheringham, S. J., & Vigroux, L. 1986, *ApJ*, 306, 110
- Franceschini, A., Braitto, V., Persic, M., et al. 2003, *MNRAS*, 343, 1181
- Gallego, J., Zamorano, J., Rego, M., Alonso, O., & Vitores, A. G. 1996, *A&AS*, 120, 323
- Garland, C. A., Pisano, D. J., Williams, J. P., Guzmán, R., & Castander, F. J. 2004, *ApJ*, 615, 689
- Garland, C. A., Williams, J. P., Pisano, D. J., et al. 2005, *ApJ*, 624, 714
- Genzel, R., Tacconi, L. J., Rigopoulou, D., Lutz, D., & Tecza, M. 2001, *ApJ*, 563, 527
- Genzel, R., Tacconi, L. J., Combes, F., et al. 2012, *ApJ*, 746, 69
- Georgakakis, A., Hopkins, A. M., Caulton, A., et al. 2001, *MNRAS*, 326, 1431
- Gonçalves, A. C., Véron-Cetty, M.-P., & Véron, P. 1999, *A&AS*, 135, 437
- Goudfrooij, P., Hansen, L., Jorgensen, H. E., & Norgaard-Nielsen, H. U. 1994, *A&AS*, 105, 341
- Graham, A. W., & Worley, C. C. 2008, *MNRAS*, 388, 1708
- Haan, S., Surace, J. A., Armus, L., et al. 2011, *AJ*, 141, 100
- Hattori, T., Yoshida, M., Ohtani, H., et al. 2004, *AJ*, 127, 736
- Helfer, T. T., Thornley, M. D., Regan, M. W., et al. 2003, *ApJS*, 145, 259
- Helou, G., Khan, I. R., Malek, L., & Boehmer, L. 1988, *ApJS*, 68, 151
- Helou, G., Soifer, B. T., & Rowan-Robinson, M. 1985, *ApJ*, 298, L7
- Hernquist, L. 1989, *Nature*, 340, 687
- Hibbard, J. E., Guhathakurta, P., van Gorkom, J. H., & Schweizer, F. 1994, *AJ*, 107, 67

- Hibbard, J. E., & Mihos, J. C. 1995, *AJ*, 110, 140
- Holmberg, E. 1941, *ApJ*, 94, 385
- Holtzman, J. A., Watson, A. M., Mould, J. R., et al. 1996, *AJ*, 112, 416
- Hopkins, P. F., Cox, T. J., Younger, J. D., & Hernquist, L. 2009, *ApJ*, 691, 1168
- Hopkins, P. F., Somerville, R. S., Hernquist, L., et al. 2006, *ApJ*, 652, 864
- Horellou, C., & Booth, R. 1997, *A&AS*, 126, 3
- Howell, J. H., Armus, L., Mazzarella, J. M., et al. 2010, *ApJ*, 715, 572
- Hubble, E. 1958, *The realm of the nebulae* (New York: Dover, 1958)
- Hubble, E. P. 1936, *Realm of the Nebulae* (New Haven: Yale University Press, 1936)
- Huchtmeier, W. K., & Tammann, G. A. 1992, *A&A*, 257, 455
- Hunt, L. K., Combes, F., García-Burillo, S., et al. 2008, *A&A*, 482, 133
- Imanishi, M. 2006, *AJ*, 131, 2406
- Imanishi, M., Nakagawa, T., Shirahata, M., Ohyama, Y., & Onaka, T. 2010, *ApJ*, 721, 1233
- Imanishi, M., Terashima, Y., Anabuki, N., & Nakagawa, T. 2003, *ApJ*, 596, L167
- Immeli, A., Samland, M., Gerhard, O., & Westera, P. 2004, *A&A*, 413, 547
- Iono, D., Yun, M. S., & Mihos, J. C. 2004, *ApJ*, 616, 199
- Iono, D., Wilson, C. D., Yun, M. S., et al. 2009, *ApJ*, 695, 1537
- Iwasawa, K., Sanders, D. B., Teng, S. H., et al. 2011, *A&A*, 529, A106
- James, P., Bate, C., Wells, M., Wright, G., & Doyon, R. 1999, *MNRAS*, 309, 585
- Jarrett, T. H., Chester, T., Cutri, R., Schneider, S. E., & Huchra, J. P. 2003, *AJ*, 125, 525
- Ji, L., Chen, Y., Huang, J. H., Gu, Q. S., & Lei, S. J. 2000, *A&A*, 355, 922
- Jog, C. J., & Chitre, A. 2002, *A&A*, 393, L89

## BIBLIOGRAPHY

---

- Jogee, S., Miller, S. H., Penner, K., et al. 2009, *ApJ*, 697, 1971
- Jütte, E., Aalto, S., & Hüttemeister, S. 2010, *A&A*, 509, A19
- Kennicutt, Jr., R. C. 1998, *ARA&A*, 36, 189
- Kennicutt, Jr., R. C., Armus, L., Bendo, G., et al. 2003, *PASP*, 115, 928
- Kereš, D., Katz, N., Weinberg, D. H., & Davé, R. 2005, *MNRAS*, 363, 2
- Kewley, L. J., Heisler, C. A., Dopita, M. A., & Lumsden, S. 2001, *ApJS*, 132, 37
- Kim, D.-W., Jura, M., Guhathakurta, P., Knapp, G. R., & van Gorkom, J. H. 1988, *ApJ*, 330, 684
- Knapen, J. H. 2005, *A&A*, 429, 141
- Koda, J., Sofue, Y., Kohno, K., et al. 2002, *ApJ*, 573, 105
- König, S., Aalto, S., Muller, S., Beswick, R. J., & Gallagher, J. S. 2013, *A&A*, 553, A72
- Koribalski, B. S., Staveley-Smith, L., Kilborn, V. A., et al. 2004, *AJ*, 128, 16
- Kormendy, J., & Bender, R. 1996, *ApJ*, 464, L119
- Laine, S., van der Marel, R. P., Rossa, J., et al. 2003, *AJ*, 126, 2717
- Lake, G., & Dressler, A. 1986, *ApJ*, 310, 605
- Larson, R. B., & Tinsley, B. M. 1978, *ApJ*, 219, 46
- Lees, J. F., Knapp, G. R., Rupen, M. P., & Phillips, T. G. 1991, *ApJ*, 379, 177
- Lin, L., Patton, D. R., Koo, D. C., et al. 2008, *ApJ*, 681, 232
- Longhetti, M., Rampazzo, R., Bressan, A., & Chiosi, C. 1998, *A&AS*, 130, 267
- Lonsdale, C. J., Lonsdale, C. J., Smith, H. E., & Diamond, P. J. 2003, *ApJ*, 592, 804
- Maiolino, R., Ruiz, M., Rieke, G. H., & Papadopoulos, P. 1997, *ApJ*, 485, 552
- Malin, D. F., & Carter, D. 1983, *ApJ*, 274, 534
- Manthey, E., Aalto, S., Hüttemeister, S., & Oosterloo, T. A. 2008, *A&A*, 484, 693



- Mao, R.-Q., Schulz, A., Henkel, C., et al. 2010, *ApJ*, 724, 1336
- Marino, A., Iodice, E., Tantalò, R., et al. 2009, *A&A*, 508, 1235
- Márquez, I., Masegosa, J., Moles, M., et al. 2002, *A&A*, 393, 389
- Martini, P., Regan, M. W., Mulchaey, J. S., & Pogge, R. W. 2003, *ApJS*, 146, 353
- McGaugh, S. S., & Bothun, G. D. 1990, *AJ*, 100, 1073
- Mihos, C. 1999, *Ap&SS*, 266, 195
- Mihos, J. C., & Bothun, G. D. 1998, *ApJ*, 500, 619
- Mihos, J. C., Bothun, G. D., & Richstone, D. O. 1993, *ApJ*, 418, 82
- Mihos, J. C., & Hernquist, L. 1996, *ApJ*, 464, 641
- Miller, B. W., Whitmore, B. C., Schweizer, F., & Fall, S. M. 1997, *AJ*, 114, 2381
- Minkowski, R. L., & Abell, G. O. 1963, *The National Geographic Society-Palomar Observatory Sky Survey* (the University of Chicago Press), 481
- Mirabel, I. F., Booth, R. S., Johansson, L. E. B., Garay, G., & Sanders, D. B. 1990, *A&A*, 236, 327
- Mirabel, I. F., & Sanders, D. B. 1988, *ApJ*, 335, 104
- Moshir, M., Kopman, G., & Conrow, T. A. O. 1992, *IRAS Faint Source Survey, Explanatory supplement version 2* (Pasadena: Infrared Processing and Analysis Center, California Institute of Technology, 1992, edited by Moshir, M.; Kopman, G.; Conrow, T. a.o.)
- Moshir, M., Kopan, G., Conrow, T., et al. 2008, *VizieR Online Data Catalog*, 2275, 0
- Mulchaey, J. S., Wilson, A. S., & Tsvetanov, Z. 1996, *ApJS*, 102, 309
- Murray, N., & Rahman, M. 2010, *ApJ*, 709, 424
- Naab, T., & Burkert, A. 2001, in *Astronomical Society of the Pacific Conference Series*, Vol. 249, *The Central Kiloparsec of Starbursts and AGN: The La Palma Connection*, ed. J. H. Knapen, J. E. Beckman, I. Shlosman, & T. J. Mahoney, 735

## BIBLIOGRAPHY

---

- Naab, T., & Burkert, A. 2003, *ApJ*, 597, 893
- Naab, T., Johansson, P. H., & Ostriker, J. P. 2009, *ApJ*, 699, L178
- Naab, T., Khochfar, S., & Burkert, A. 2006, *ApJ*, 636, L81
- Nagao, T., Taniguchi, Y., & Murayama, T. 2000, *AJ*, 119, 2605
- Nakajima, T., Sakai, T., Asayama, S., et al. 2008, *PASJ*, 60, 435
- Nakanishi, H., & Sofue, Y. 2006, *PASJ*, 58, 847
- Narayanan, D., Bothwell, M., & Davé, R. 2012a, *MNRAS*, 426, 1178
- Narayanan, D., Cox, T. J., & Hernquist, L. 2008, *ApJ*, 681, L77
- Narayanan, D., Groppi, C. E., Kulesa, C. A., & Walker, C. K. 2005, *ApJ*, 630, 269
- Narayanan, D., Krumholz, M. R., Ostriker, E. C., & Hernquist, L. 2012b, *MNRAS*, 421, 3127
- Neugebauer, G., Habing, H. J., van Duinen, R., et al. 1984, *ApJ*, 278, L1
- Nicholson, R. A., Bland-Hawthorn, J., & Taylor, K. 1992, *ApJ*, 387, 503
- Nilson, P. 1973, *Uppsala general catalogue of galaxies (Acta Universitatis Upsaliensis. Nova Acta Regiae Societatis Scientiarum Upsaliensis - Uppsala Astronomiska Observatoriums Annaler, Uppsala: Astronomiska Observatorium, 1973)*
- Osterbrock, D. E., & Martel, A. 1993, *ApJ*, 414, 552
- Papadopoulos, P. P., van der Werf, P., Xilouris, E., Isaak, K. G., & Gao, Y. 2012, *ApJ*, 751, 10
- Peebles, M. S., & Martini, P. 2006, *ApJ*, 652, 1097
- Penzias, A. A., & Wilson, R. W. 1965, *ApJ*, 142, 419
- Poggianti, B. M., & Wu, H. 2000, *ApJ*, 529, 157
- Quinn, P. J., Hernquist, L., & Fullagar, D. P. 1993, *ApJ*, 403, 74
- Rampazzo, R., Plana, H., Longhetti, M., et al. 2003, *MNRAS*, 343, 819

- Rampazzo, R., Marino, A., Tantalò, R., et al. 2007, *MNRAS*, 381, 245
- Regan, M. W., Thornley, M. D., Helfer, T. T., et al. 2001, *ApJ*, 561, 218
- Richter, O.-G., Sackett, P. D., & Sparke, L. S. 1994, *AJ*, 107, 99
- Rigopoulou, D., Lawrence, A., White, G. J., Rowan-Robinson, M., & Church, S. E. 1996, *A&A*, 305, 747
- Risaliti, G., Maiolino, R., Marconi, A., et al. 2006, *MNRAS*, 365, 303
- Robertson, B. E., & Bullock, J. S. 2008, *ApJ*, 685, L27
- Rothberg, B., & Fischer, J. 2010, *ApJ*, 712, 318
- Rothberg, B., & Joseph, R. D. 2004, *AJ*, 128, 2098
- . 2006a, *AJ*, 131, 185
- . 2006b, *AJ*, 132, 976
- Sanders, D. B., & Mirabel, I. F. 1996, *ARA&A*, 34, 749
- Sanders, D. B., Scoville, N. Z., & Soifer, B. T. 1991, *ApJ*, 370, 158
- Schimminovich, D. 2001, in *Astronomical Society of the Pacific Conference Series*, Vol. 240, *Gas and Galaxy Evolution*, ed. J. E. Hibbard, M. Rupen, & J. H. van Gorkom, 147
- Schimminovich, D., van Gorkom, J. H., & van der Hulst, J. M. 2013, *AJ*, 145, 34
- Schombert, J. M., Wallin, J. F., & Struck-Marcell, C. 1990, *AJ*, 99, 497
- Schweizer, F. 1982, *ApJ*, 252, 455
- Schweizer, F. 1983, in *IAU Symposium*, Vol. 100, *Internal Kinematics and Dynamics of Galaxies*, ed. E. Athanassoula, 319–326
- . 1986, *Science*, 231, 227
- Schweizer, F. 1990, in *Dynamics and Interactions of Galaxies*, ed. R. Wielen, 60–71
- . 1996, *AJ*, 111, 109

## BIBLIOGRAPHY

---

- Schweizer, F., & Seitzer, P. 1992, *AJ*, 104, 1039
- . 2007, *AJ*, 133, 2132
- Sekiguchi, K., & Wolstencroft, R. D. 1993, *MNRAS*, 263, 349
- Shier, L. M., & Fischer, J. 1998, *ApJ*, 497, 163
- Simien, F., & Prugniel, P. 1997, *A&AS*, 122, 521
- Sliwa, K., Wilson, C. D., Petitpas, G. R., et al. 2012, *ApJ*, 753, 46
- Smirnova, A., & Moiseev, A. 2010, *MNRAS*, 40, 307
- Smith, D. A., Herter, T., Haynes, M. P., Beichman, C. A., & Gautier, III, T. N. 1996, *ApJS*, 104, 217
- Smith, E. P., & Hintzen, P. 1991, *AJ*, 101, 410
- Smith, H. E., Lonsdale, C. J., & Lonsdale, C. J. 1998, *ApJ*, 492, 137
- Smoot, G. F., Bennett, C. L., Kogut, A., et al. 1992, *ApJ*, 396, L1
- Solomon, P. M., & Barrett, J. W. 1991, in *IAU Symposium, Vol. 146, Dynamics of Galaxies and Their Molecular Cloud Distributions*, ed. F. Combes & F. Casoli, 235
- Solomon, P. M., Downes, D., Radford, S. J. E., & Barrett, J. W. 1997, *ApJ*, 478, 144
- Solomon, P. M., & Vanden Bout, P. A. 2005, *ARA&A*, 43, 677
- Springel, V., Di Matteo, T., & Hernquist, L. 2005, *ApJ*, 620, L79
- Springel, V., & Hernquist, L. 2005, *ApJ*, 622, L9
- Springob, C. M., Haynes, M. P., Giovanelli, R., & Kent, B. R. 2005, *ApJS*, 160, 149
- Struck, C. 1999, *Phys. Rep.*, 321, 1
- Tacconi, L. J., Genzel, R., Smail, I., et al. 2008, *ApJ*, 680, 246
- Tacconi, L. J., Genzel, R., Neri, R., et al. 2010, *Nature*, 463, 781
- Tacconi, L. J., Neri, R., Genzel, R., et al. 2013, *ApJ*, 768, 74

- Takeuchi, T. T., Buat, V., Heinis, S., et al. 2010, *A&A*, 514, A4
- Taniguchi, Y., & Noguchi, M. 1991, *AJ*, 101, 1601
- Theureau, G., Bottinelli, L., Coudreau-Durand, N., et al. 1998, *A&AS*, 130, 333
- Tielens, A. G. G. M. 2005, *The Physics and Chemistry of the Interstellar Medium* (Cambridge, UK: Cambridge University Press, 2005)
- Toomre, A. 1977, in *Evolution of Galaxies and Stellar Populations*, ed. B. M. Tinsley & R. B. G. Larson, D. Campbell, 401
- Toomre, A., & Toomre, J. 1972, *ApJ*, 178, 623
- Ueda, J., Iono, D., Petitpas, G., et al. 2012, *ApJ*, 745, 65
- Veilleux, S., Kim, D.-C., Sanders, D. B., Mazzarella, J. M., & Soifer, B. T. 1995, *ApJS*, 98, 171
- Vorontsov-Velyaminov, B. A. 1959, in *Atlas and catalog of interacting galaxies (1959)*, 0
- Vorontsov-Velyaminov, B. A. 1977, *A&AS*, 28, 1
- Walker, I. R., Mihos, J. C., & Hernquist, L. 1996, *ApJ*, 460, 121
- Wang, Z., Schweizer, F., & Scoville, N. Z. 1992, *ApJ*, 396, 510
- Wang, Z., Scoville, N. Z., & Sanders, D. B. 1991, *ApJ*, 368, 112
- Weil, M. L., Bland-Hawthorn, J., & Malin, D. F. 1997, *ApJ*, 490, 664
- Whitmore, B. C., Lucas, R. A., McElroy, D. B., et al. 1990, *AJ*, 100, 1489
- Whitmore, B. C., Miller, B. W., Schweizer, F., & Fall, S. M. 1997, *AJ*, 114, 1797
- Whitmore, B. C., Schweizer, F., Leitherer, C., Borne, K., & Robert, C. 1993, *AJ*, 106, 1354
- Wiklind, T., Combes, F., & Henkel, C. 1995, *A&A*, 297, 643
- Wilson, C. D. 1995, *ApJ*, 448, L97
- Wilson, C. D., Petitpas, G. R., Iono, D., et al. 2008, *ApJS*, 178, 189

## ACKNOWLEDGE

---

- Wright, A., & Otrupcek, R. 1992, Bulletin d'Information du Centre de Donnees Stellaires, 41, 47
- Yamamura, I., Makiuti, S., Ikeda, N., et al. 2010, VizieR Online Data Catalog, 2298, 0
- Yao, L., Seaquist, E. R., Kuno, N., & Dunne, L. 2003, ApJ, 588, 771
- Young, J. S., Xie, S., Tacconi, L., et al. 1995, ApJS, 98, 219
- Young, L. M., Bureau, M., & Cappellari, M. 2008, ApJ, 676, 317
- Young, L. M., Bureau, M., Davis, T. A., et al. 2011, MNRAS, 414, 940
- Yuan, T.-T., Kewley, L. J., & Sanders, D. B. 2010, ApJ, 709, 884
- Yun, M. S., Ho, P. T. P., & Lo, K. Y. 1994, Nature, 372, 530
- Yun, M. S., Reddy, N. A., & Condon, J. J. 2001, ApJ, 554, 803
- Zhu, M., Seaquist, E. R., Davoust, E., Frayer, D. T., & Bushouse, H. A. 1999, AJ, 118, 145
- Zhu, M., Seaquist, E. R., & Kuno, N. 2003, ApJ, 588, 243